# Effect of Fermented Fish Oil on Fine Particulate Matter-Induced Skin Aging

Yu Jae Hyun [1], Mei Jing Piao [1], Kyoung Ah Kang [1], Ao Xuan Zhen [1],
Pincha Devage Sameera Madushan Fernando [1], Hee Kyoung Kang [1],
Yong Seok Ahn [2] and Jin Won Hyun [1,*]

[1] School of Medicine, Jeju National University, Jeju 63243, Korea; yujae_1113@naver.com (Y.J.H.);
  meijing0219@hotmail.com (M.J.P.); legna48@hanmail.net (K.A.K.); zhenaoxuan705@gmail.com (A.X.Z.);
  sameeramadhu91@gmail.com (P.D.S.M.F.); pharmkhk@jejunu.ac.kr (H.K.K.)
[2] Choung Ryong Fisheries Co. LTD, 7825 Iljudong-ro, Namwon-epu, Seogwipo, Jeju 63612, Korea;
  ecoil@daum.net
*  Correspondence: jinwonh@jejunu.ac.kr; Tel.: +82-64-754-3838

check for updates

**Abstract:** Skin is exposed to various harmful environmental factors such as air pollution, which includes different types of particulate matter (PM). Atmospheric PM has harmful effects on humans through increasing the generation of reactive oxygen species (ROS), which have been reported to promote skin aging via the induction of matrix metalloproteinases (MMPs), which in turn can cause the degradation of collagen. In this study, we investigated the effect of fermented fish oil (FFO) derived from mackerel on fine PM (particles with a diameter < 2.5 μm: $PM_{2.5}$)-induced skin aging in human keratinocytes. We found that FFO inhibited the $PM_{2.5}$-induced generation of intracellular ROS and MMPs, including MMP-1, MMP-2, and MMP-9. In addition, FFO significantly abrogated the elevation of intracellular $Ca^{2+}$ levels in $PM_{2.5}$-treated cells and was also found to block the $PM_{2.5}$-induced mitogen-activated protein kinase/activator protein 1 (MAPK/AP-1) pathway. In conclusion, FFO has an anti-aging effect on $PM_{2.5}$-induced aging in human keratinocytes.

**Keywords:** particulate matter; matrix metalloproteinase; fermented fish oil; oxidative stress; skin aging

## 1. Introduction

Reactive oxygen species (ROS) have unpaired electrons and unstable bonds, which are properties that can lead to cellular damage [1,2] and the regulation transcription factors such as AP-1 and NF-kB [3,4]. Cellular ROS can accumulate in response to exogenous stimuli, including air pollution [4].

The skin is the largest organ in the human body and acts as the first-line defense barrier against harmful stimuli such as ultraviolet (UV) light and air pollution, including particulate matter (PM). Depending on particle size, PM can be classified as ultrafine (particles with a diameter < 0.1 μm: $PM_{0.1}$), fine (particles with a diameter < 2.5 μm: $PM_{2.5}$), and coarse (particles with a diameter < 10 μm: $PM_{10}$) [5]. PM can lead to the development of various skin diseases, including skin aging, alopecia, and skin cancer, through the induction of oxidative stress [6,7]. In addition, PM-induced oxidative stress promoted via the production of ROS and subsequent increase in the activity of matrix metalloproteinases (MMPs) [6,8], including MMP-1, MMP-2, and MMP-9, can cause skin aging as a consequence of the degradation of collagen [9,10].

The generation of ROS has been reported to affect skin aging by increasing the expression of MMP-1 in keratinocytes [11]. Several studies have reported that UVB-induced ROS causes skin photoaging via the promotion of the activity of MMP-1 in human keratinocytes and dermal

fibroblasts [12,13], and accordingly, it would be desirable to identify an effective antioxidant that could be used to prevent skin aging.

Oxidative stress is also known to stimulate mitogen-activated protein kinase (MAPK) signaling pathways, which affect the regulation mediated by transcription factor activator protein 1 (AP-1) [14]. Activated (phosphorylated) c-Jun and c-Fos can comprise homodimers or heterodimers that bind to AP-1 binding sites in the promoter region of target genes to promote gene transcription [15] such as that of MMPs [10].

Although previous studies have reported that fermented fish oil (FFO) has an antioxidant and protective effect against UVB-induced oxidative damage [16], the effects of FFO on $PM_{2.5}$-induced skin aging are poorly understood. Therefore, in this study, to gain further insight into the antioxidative properties of FFO we investigated the effects of this oil on $PM_{2.5}$-induced skin aging.

## 2. Results

### 2.1. Effect of FFO on $PM_{2.5}$-Induced Intracellular ROS

Given that ROS has been reported to affect skin aging via the generation of MMPs [11], we measured the generation of intracellular ROS using 2′,7′-dichlorodihydrofluorescein diacetate (DCF-DA) fluorescence dye. The flow cytometry data indicated that $PM_{2.5}$-treated cells induced ROS and that pretreatment with FFO reduced $PM_{2.5}$-induced ROS in HaCaT cells, which was confirmed by confocal microscopy (Figure 1a,b).
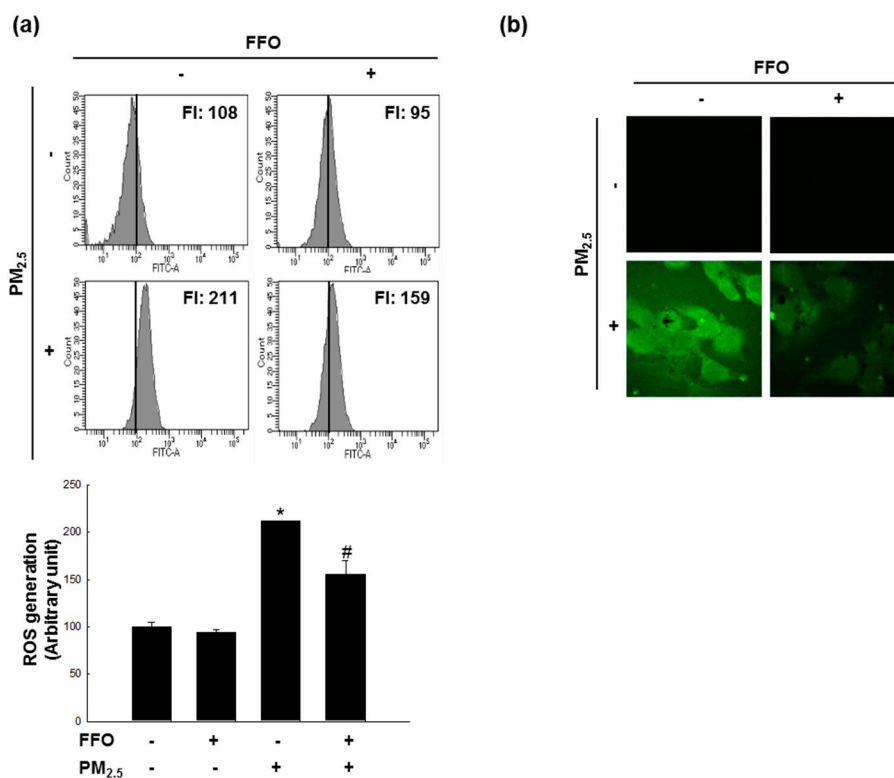


**Figure 1.** Scavenging effect of fermented fish oil (FFO) on $PM_{2.5}$-induced intracellular reactive oxygen species (ROS). Intracellular ROS were detected by (**a**) flow cytometry and (**b**) confocal microscopy after DCF-DA staining. * $p < 0.05$ and # $p < 0.05$ compared with untreated cells and $PM_{2.5}$-treated cells, respectively.

## 2.2. PM$_{2.5}$-Induced Keratinocyte Senescence

Next, we measured β-galactosidase activity, a marker of cellular senescence [17], to detect HaCaT cell senescence using flow cytometry and confocal microscopy after SPiDER-βGal staining. PM$_{2.5}$-treated cells showed increased β-galactosidase activity in the cytosol, whereas FFO treatment was found to decrease the PM$_{2.5}$-induced β-galactosidase activity (Figure 2a,b).
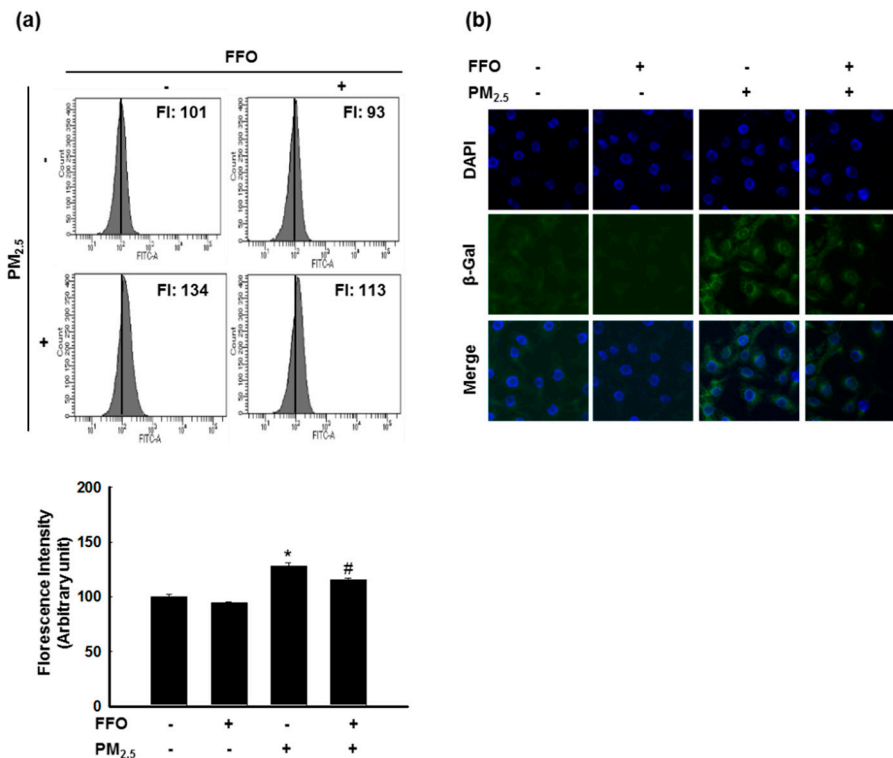


**Figure 2.** PM$_{2.5}$-induced keratinocyte senescence. (**a**) β-galactosidase activity was measured by flow cytometry and (**b**) confocal microscopy after SPiDER-βGal staining. * $p < 0.05$ and # $p < 0.05$ compared with untreated cells and PM$_{2.5}$-treated cells, respectively.

## 2.3. Effect of FFO on PM$_{2.5}$-Induced MMP-1 Activation and MMP Expression

In this study, we examined cellular MMP-1 activity, as MMP-1 is known to be primarily responsible for skin aging via collagen degradation [18]. The treatment of cells with PM$_{2.5}$ significantly increased the activation of MMP-1 after 6, 12, and 24 h (Figure 3a), whereas pretreatment with FFO decreased the PM$_{2.5}$-induced activation of MMP-1 (Figure 3b). The expression of MMP-1 mRNA and protein was also increased in PM$_{2.5}$-treated cells, whereas it was decreased in the cells pretreated with FFO (Figure 3c,d). As MMP-2 and MMP-9 have also been reported to be involved in skin aging through the degradation of collagen [19], we analyzed the expression levels of MMP-2 and MMP-9 protein and found that these were also increased by PM$_{2.5}$ treatment and decreased by FFO pretreatment (Figure 3e).
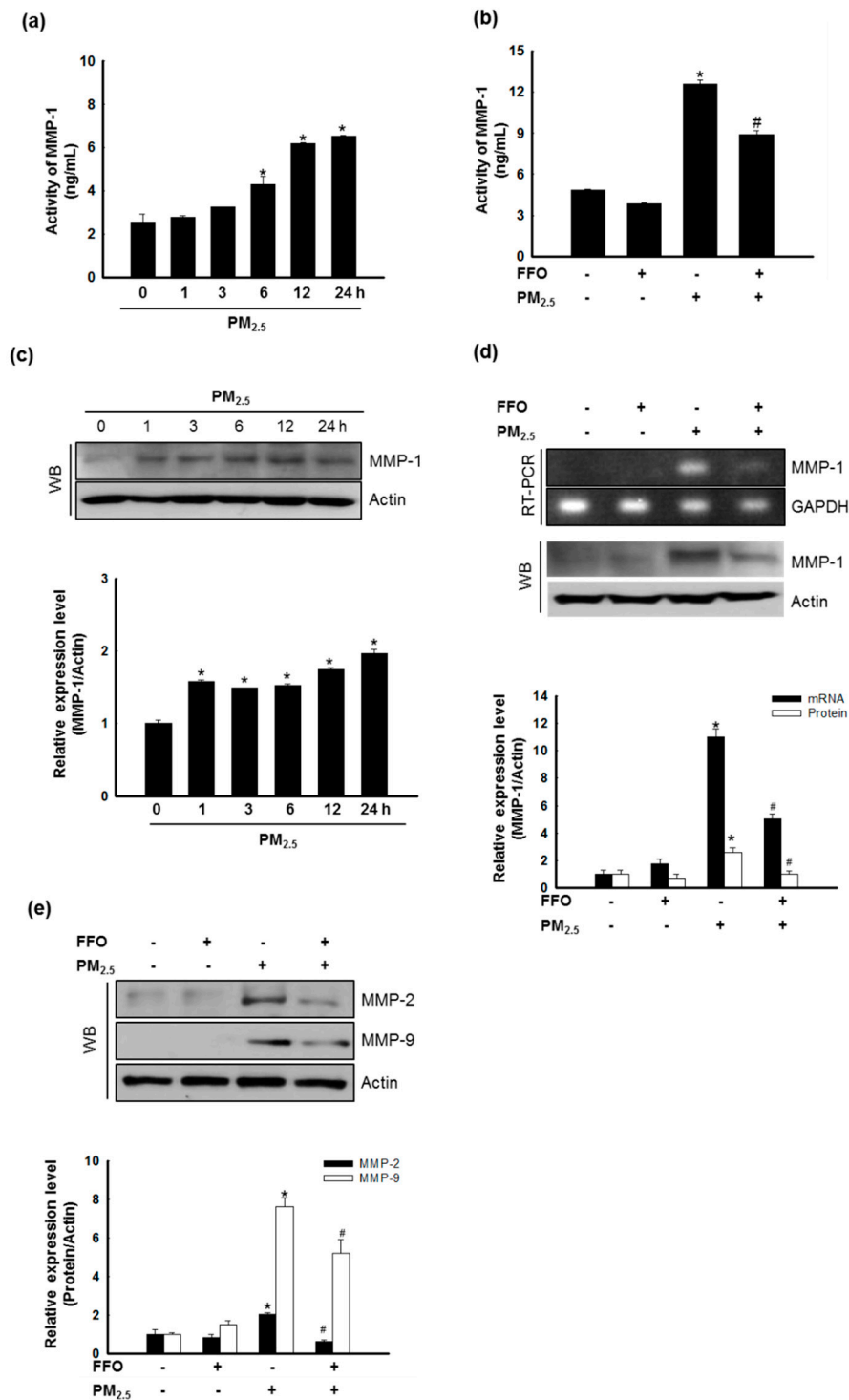
**Figure 3.** Effect of fermented fish oil (FFO) on $PM_{2.5}$-induced MMP-1 activation and matrix metalloproteinase (MMP) expression. (**a**) The MMP-1 activity of $PM_{2.5}$-treated cells at the indicated times and (**b**) the MMP-1 activity of FFO and $PM_{2.5}$ treated cells were determined using a human active MMP-1 fluorescent assay kit. * $p < 0.05$ and # $p < 0.05$ compared with untreated cells and $PM_{2.5}$-treated cells, respectively. (**c**) Expression level of MMP-1 was analyzed by western blot analysis. Actin was used as a loading control. * $p < 0.05$ compared with untreated cells. (**d**) The mRNA and protein levels of MMP-1 were analyzed by RT-PCR and western blotting, respectively. GAPDH and actin were used as loading controls. * $p < 0.05$ and # $p < 0.05$ compared with untreated cells and $PM_{2.5}$-treated cells, respectively. (**e**) Expression level of MMP-2 and MMP-9 were analyzed by western blotting. Actin was used as a loading control. * $p < 0.05$ and # $p < 0.05$ compared with untreated cells and $PM_{2.5}$-treated cells, respectively.

## 2.4. Effect of FFO on PM$_{2.5}$-Induced MAPKs and Intracellular Ca$^{2+}$ Levels

MAPKs, which enhance the expression of MMP-1, are activated by an increase in the intracellular Ca$^{2+}$ levels [20]. Our western blot analysis indicated that PM$_{2.5}$ treatment induced the activation (phosphorylation) of extracellular signal-regulated kinase (ERK) and c-Jun N-terminal kinase (JNK), whereas this activation was decreased following FFO pretreatment. Furthermore, PM$_{2.5}$ treatment induced the activation (phosphorylation) of MAPK kinase (MEK) 1/2 and SAPK/ERK kinase (SEK) 1 (Figure 4a), and significantly increased the levels of intracellular Ca$^{2+}$, whereas FFO decreased the PM$_{2.5}$-induced increase in Ca$^{2+}$ levels (Figure 4b,c).
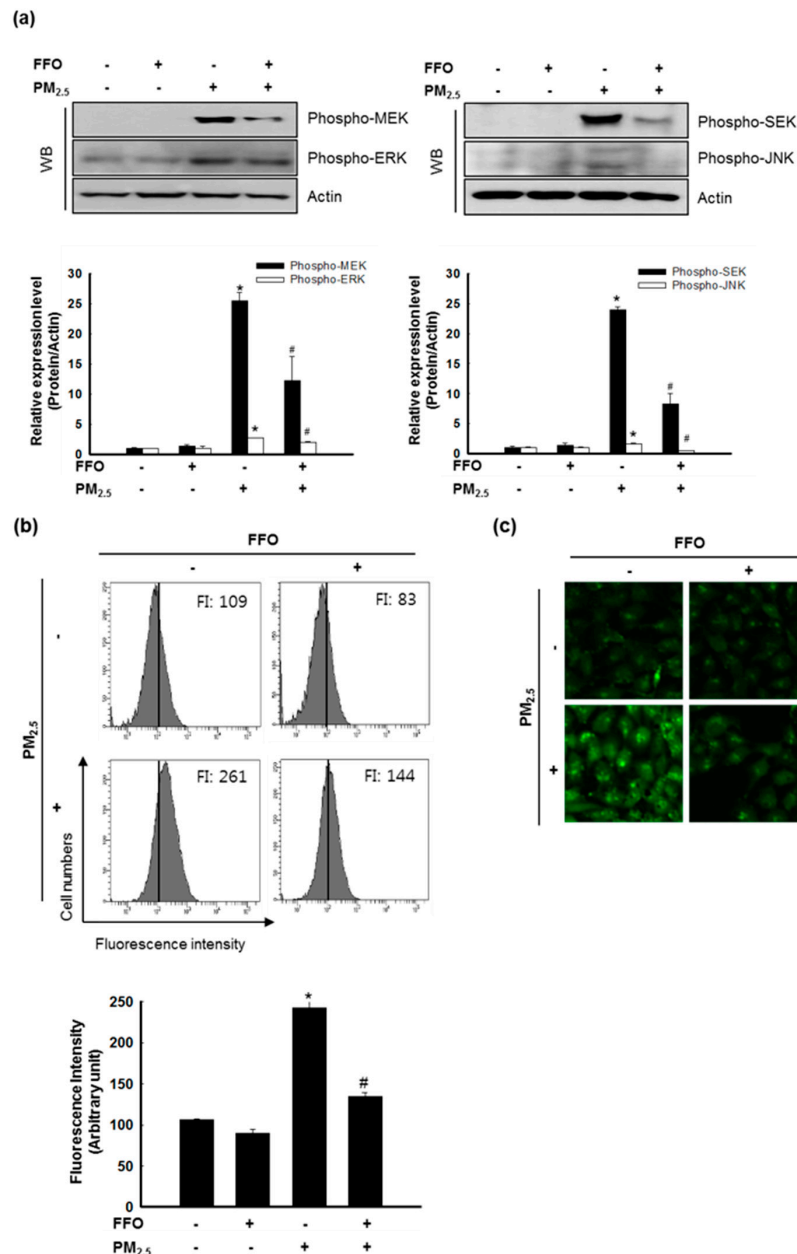


**Figure 4.** Effect of fermented fish oil (FFO) on PM$_{2.5}$-induced MAPKs and intracellular Ca$^{2+}$ level. (**a**) Expression level of phospho-MEK, phospho-ERK, phospho-SEK, and phospho-JNK determined by western blot analysis. Actin was used as a loading control. * $p < 0.05$ and # $p < 0.05$ compared with untreated cells and PM$_{2.5}$-treated cells, respectively. (**b**) Intracellular Ca$^{2+}$ level was detected by flow cytometry and (**c**) confocal microscopy after Flou-4-AM staining. * $p < 0.05$ and # $p < 0.05$ compared with untreated cells and PM$_{2.5}$-treated cells, respectively.

## 2.5. Effect of FFO on PM$_{2.5}$-Induced Transcription Factor Activator Protein 1 (AP-1) Expression

The nuclear transcription factor, AP-1, regulated by MAPKs, increases the expression of MMPs [12,21]. The activation of MAPKs results in the heterodimerization of c-Jun/c-Fos and the formation of an AP-1 complex [10]. As shown in Figure 4, PM$_{2.5}$ treatment increased MAPK activity and intracellular Ca$^{2+}$ levels. Western blot analysis of c-Fos and phospho-c-Jun levels indicated that FFO significantly decreased the PM$_{2.5}$-induced increase in phospho-c-Jun and c-Fos levels (Figure 5a). In addition, FFO reduced the PM$_{2.5}$-induced AP-1 binding to the MMP-1 promoter (Figure 5b).
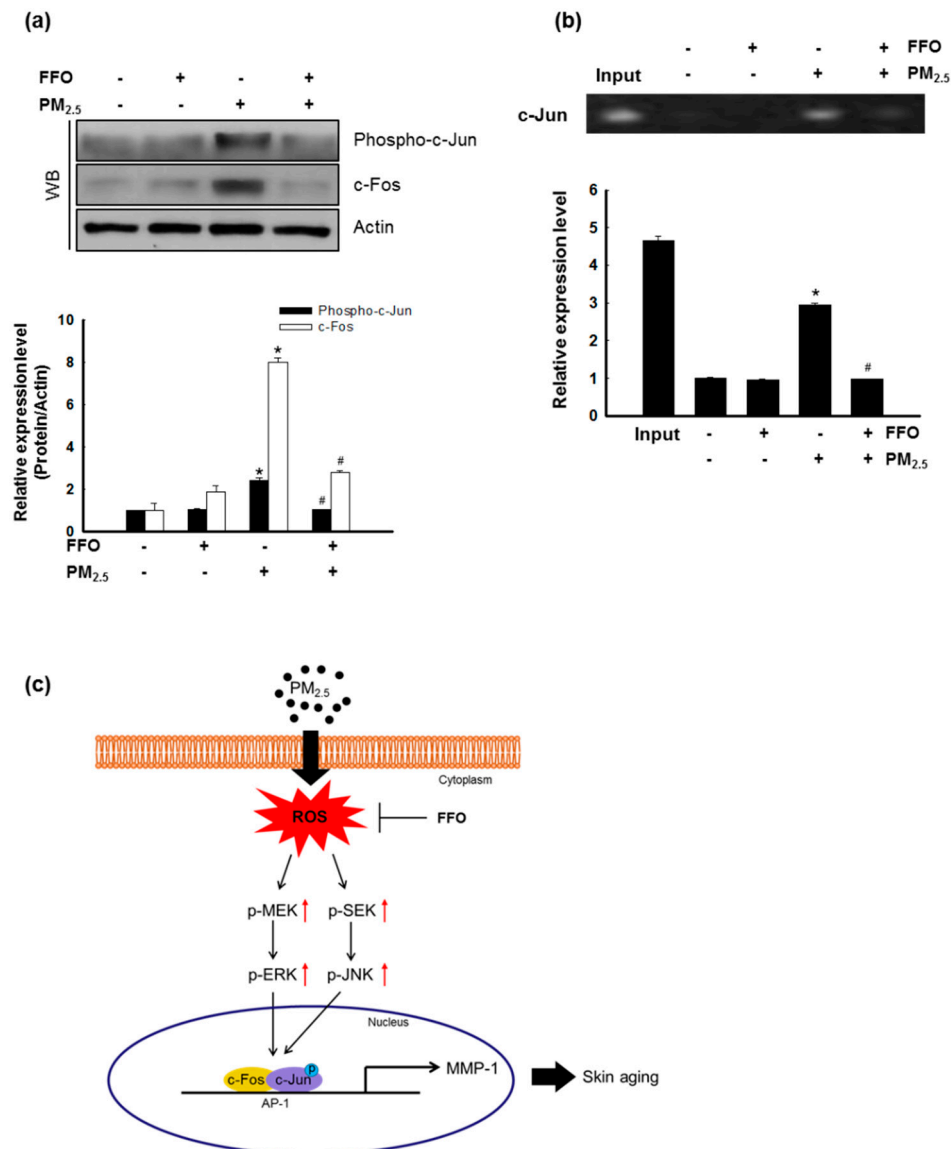


**Figure 5.** Effect of fermented fish oil (FFO) on PM$_{2.5}$-induced transcription factor activator protein 1 (AP-1) expression. (**a**) Expression level of phospho-c-Jun and c-Fos determined by western blot analysis. Actin was used as a loading control. * $p < 0.05$ and # $p < 0.05$ compared with untreated cells and PM$_{2.5}$-treated cells, respectively. (**b**) AP-1 binding to the MMP-1 promoter was assessed by ChIP assay. * $p < 0.05$ and # $p < 0.05$ compared with untreated cells and PM$_{2.5}$-treated cells, respectively. (**c**) Schematic diagram of the effect of FFO on PM$_{2.5}$-induced skin aging. Exposure to PM$_{2.5}$ increased intracellular reactive oxygen species (ROS) and induced skin aging in HaCaT cells. The mackerel-derived FFO had an anti-aging effect on PM$_{2.5}$-induced skin aging through reduced intracellular ROS.

## 3. Discussion

The skin is the largest organ in the human body and acts as a first-line defense barrier against harmful environmental stimuli, including PM. In several studies, $PM_{2.5}$ has been reported to have harmful effects associated with inflammatory skin diseases, skin aging, and damage to the respiratory system through the generation of intracellular ROS [6,22,23]. The accumulation of ROS has been reported to induce skin aging through the expression of MMPs, including MMP-1, MMP-2, and MMP-9 [24]. Accordingly, it is desirable to identify an effective antioxidant that could be used to prevent skin aging.

Previous studies have demonstrated that mackerel-derived FFO has a direct ROS scavenging effect and a protective effect against UVB-induced oxidative damage [16]. In the present study, we focused on the effect of mackerel-derived FFO against $PM_{2.5}$-induced skin aging.

We initially measured the generation of intracellular ROS induced by $PM_{2.5}$ treatment, and accordingly found that pretreatment with FFO significantly reduced the induction of intracellular ROS by $PM_{2.5}$ treatment (Figure 1a,b). Given that the generation of ROS causes skin aging, we investigated keratinocyte senescence by examining the activity of the marker enzyme β-galactosidase [25]. We found that $PM_{2.5}$ treatment increased β-galactosidase activity, whereas FFO pretreatment significantly reduced the $PM_{2.5}$-induced β-galactosidase activity (Figure 2a,b). As MMPs are known to cause skin aging through the degradation of collagen [9,10], we also examined the activity of MMP-1 and the expression levels of MMP-1, MMP-2, and MMP-9. Again, we found that FFO has an inhibitory effect on $PM_{2.5}$-induced MMPs (Figure 3). These results indicate that $PM_{2.5}$ induces skin aging by promoting the expression of MMPs, whereas FFO has anti-aging effects via its ROS scavenging activity.

ROS activated MAPK signaling pathways, and the activation of MAPKs, in turn, induced various transcription factors, including AP-1 and NF-κB [14,26]. As a result of the translocation of activated AP-1, heterodimers comprising c-Jun and c-Fos and MMPs were synthesized [27,28]. As shown in Figure 4a, ERK and JNK were activated by $PM_{2.5}$ treatment, and this activation was reduced by FFO pretreatment. The activation of MEK and SEK, upstream of ERK and JNK, respectively, was also increased by $PM_{2.5}$ treatment, and this increase was again decreased by FFO pretreatment (Figure 4a). In addition, intracellular $Ca^{2+}$ levels, which regulate MAPKs, were significantly increased in $PM_{2.5}$-treated cells, whereas pretreatment with FFO was found to decrease the observed $PM_{2.5}$-induced increase in $Ca^{2+}$ levels (Figure 4b,c). Furthermore, phospho-c-Jun and c-Fos levels were increased in $PM_{2.5}$-treated cells and decreased in cells receiving pretreatment with FFO (Figure 5a). We also found that $PM_{2.5}$-induced AP-1 binding to the MMP-1 promoter was reduced by FFO pretreatment (Figure 5b). These results therefore provide evidence that FFO can block the activation of the MAPK/AP-1 pathway induced by $PM_{2.5}$ in human keratinocytes. FFO showed an antioxidant effect in this study and in our previous study [16]. However, we did not assess whether FFO may induce the nuclear factor-erythroid 2-related factor 2-mediated antioxidant enzyme pathway to scavenge ROS. This will be evaluated in a future study.

In conclusion, mackerel-derived FFO has anti-aging effects against $PM_{2.5}$-induced skin aging through a reduction in the generation of intracellular ROS and expression of MMPs (Figure 5c).

## 4. Materials and Methods

### 4.1. Cell Culture and Treatment

HaCaT human keratinocytes (CLS Cell Lines Service GmbH, Eppelheim, Germany) were cultured in DMEM medium (Gibco, Life Technologies Co., Grand Island, NY, USA) supplemented with 10% fetal bovine serum and antibiotics (100 units/mL penicillin, 100 μg/mL streptomycin, and 0.25 μg/mL amphotericin B) (Gibco, Life Technologies Co., Grand Island, NY, USA) at 37 °C in an incubator with a humidified atmosphere of 5% $CO_2$. Cells were treated with 50 μg/mL diesel particulate matter NIST 1650b ($PM_{2.5}$) (Sigma-Aldrich Chemical Company, St. Louis, MO, USA) and 20 μg/mL FFO. The preparation of $PM_{2.5}$ and FFO has been described in previous studies [16,29].

### 4.2. Detection of Intracellular ROS

For the detection of intracellular ROS in HaCaT cells, the cells were seeded in 6-well culture plates at a density of $1.0 \times 10^5$ cells/well, cultured for 16 h, and treated with 20 μg/mL FFO and 50 μg/mL PM$_{2.5}$. After 30 min, 50 μM 2',7'-dichlorodihydrofluorescein diacetate (DCF-DA, Molecular Proves, Eugene, OR, USA) solution was added to the cells. After 15 min incubation at 37 °C, DCF fluorescence was measured using a BD LSRFortessa flow cytometer (PerkinElmer, Waltham, MA, USA). For imaging, cells were seeded in a 4-well glass chamber slide at a density of $1.0 \times 10^5$ cells/well, cultured for 16 h, and treated with 20 μg/mL FFO and 50 μg/mL PM$_{2.5}$. After 30 min, 50 μM DCF-DA (Molecular Proves, Eugen, OR, USA) solution was added to the cells. After 15 min incubation at 37 °C, the cells were washed 3 times with PBS. DCF fluorescence images were obtained using a FV1200 laser scanning confocal microscope (Olympus, Tokyo, Japan).

### 4.3. Detection of β-Galactosidase Activity

β-galactosidase activity is a classic marker of cellular aging [30], and we accordingly measured the activity of this enzyme to detect cell senescence. Cells were seeded in 6-well culture plates at a density of $1.0 \times 10^5$ cells/mL, and after a 16-h incubation at 37 °C, they were treated with 20 μg/mL FFO and 50 μg/mL of PM$_{2.5}$, followed by the addition of 2 μM SPiDER-βGal solution (Dojindo Molecular Technologies, Inc., Rockville, MD, USA) 24 h later. After a 15-min incubation at 37 °C, SPiDER-βGal fluorescence was measured using a BD LSRFortessa flow cytometer (PerkinElmer, Waltham, MA, USA). For imaging, cells were seeded in a 4-well glass chamber slide at a density of $1.0 \times 10^5$ cells/well, and after a 16 h incubation at 37 °C, they were treated with 20 μg/mL FFO and 50 μg/mL of PM$_{2.5}$, followed by the addition of 2 μM SPiDER-βGal solution (Dojindo Molecular Technologies, Inc., Rockville, MD, USA) 24 h later. After a 15 min incubation at 37 °C, the cells were washed 3 times with PBS. After washing, the cells were treated with mounting medium containing DAPI to label nuclei. SPiDER-βGal fluorescence images were obtained using an FV1200 laser scanning confocal microscope (Olympus, Tokyo, Japan).

### 4.4. MMP-1 Activity

MMP-1 activity was measured using a Fluorokine® E human active MMP-1 fluorescent assay kit (R&D Systems Inc., Minneapolis, MN, USA). HaCaT cells were seeded in a 60 mm culture dish at $1.0 \times 10^5$ cells/mL. After a 16 h incubation at 37 °C, the cells were treated with 20 μg/mL FFO, and 1 h thereafter with 50 μg/mL PM$_{2.5}$. MMP-1 activity was assessed according to the manufacturer's instructions. Fluorescence was measured using a Spectra Max i3x microplate reader (Molecular Devices, San Jose, CA, USA).

### 4.5. Reverse Transcription–PCR (RT-PCR)

Cells were seeded in a 60 mm culture dish at $1.5 \times 10^5$ cells/mL, and after a 1 h incubation at 37 °C, cells were treated with 20 μg/mL FFO and 50 μg/mL PM$_{2.5}$. After 24 h, we isolated total RNA from cells using an easy-BLUE™ total RNA extraction kit (iNtRON Biotechnology Inc., Seongnamsi, Korea). Subsequently, cDNA was amplified using reverse transcription reaction buffer, primers, dNTPs, and Taq DNA polymerase in a final volume of 20 μL. The amplified products were mixed with 6× blue/orange loading dye and resolved by electrophoresis on 1% agarose gels. Gels were subsequently stained with RedSafe™ nucleic acid staining solution (iNtRON Biotechnology Inc., Seongnamsi, Korea), photographed under a UV light, and analyzed using Image Quant™ TL analysis software (Amersham Biosciences, Uppsala, Sweden). The PCR conditions used were as follows: an initial denaturation at 94 °C for 5 min, followed by 30 cycles of 94 °C for 30 s, 55 °C for 30 s, and 72 °C for 1 min. The primers used in this study were as follows: human MMP-1: forward (5'-GGAGGAAATCTTGCTCAT-3') and reverse (5'-CTCAGAAAGAGCAGCATC-3'); human GAPDH: forward (5'-TCAAGTGGGGCGATGCTGGC-3') and reverse (5'-TGCCAGCCCCAGCGTCAAAG-3').

### 4.6. Western Blot Analysis

Protein lysates (30 µg per lane) were electrophoresed on 12% SDS-polyacrylamide gels, and then transferred to nitrocellulose membranes, which were incubated with the primary antibodies and subsequently with HRP-conjugated secondary antibodies (Invitrogen, Carlsbad, CA, USA). Thereafter, the membranes were developed using a western blotting detection kit (GE Healthcare Life Sciences, Buckinghamshire, Little Chalfont, UK) for detection of the protein bands and then exposed to X-ray film. The primary antibodies used in this study were as follows: MMP-1 (Cusabio Technology LLC., Houston, TX, USA), MMP-2 (Abcam, Cambridge, UK), MMP-9 (Abcam, Cambridge, UK), phospho-c-Jun (Cell Signaling Technology, Danvers, MA, USA), c-Fos (Cell Signaling Technology, Danvers, MA, USA), phospho-SEK (Cell Signaling Technology, Danvers, MA, USA), phospho-MEK (Cell signaling Technology, Danvers, MA, USA), phospho-ERK (Santa Cruz Biotechnology, Santa Cruz, CA, USA), phospho-JNK (Cell Signaling Technology, Danvers, MA, USA), and Actin (Sigma-Aldrich Chemical Company, St. Louis, MO, USA).

### 4.7. Measurement of $Ca^{2+}$ Levels

To determine cellular $Ca^{2+}$ levels, cells were seeded in 6-well culture plates at a density of $1.0 \times 10^5$ cells/well, cultured for 16 h, and then treated with 20 µg/mL FFO and 50 µg/mL $PM_{2.5}$. After 24 h, 5 µM Fluo-4-AM (Molecular Probes, Eugene, OR, USA) solution was added to the cells. After 15 min incubation at 37 °C, Fluo-4-AM fluorescence was measured using a BD LSRFortessa flow cytometer (PerkinElmer, Waltham, MA, USA). For imaging, cells were seeded in a 4-well glass chamber slide at a density of $1.0 \times 10^5$ cells/well, cultured for 16 h, and then treated with 20 µg/mL FFO and 50 µg/mL $PM_{2.5}$. After 24 h, 5 µM Fluo-4-AM (Molecular Probes, Eugen, OR, USA) solution was added to the cells. After a 15 min incubation at 37 °C, the cells were washed 3 times with PBS. After washing, Flou-4-AM fluorescence images were obtained using an FV1200 laser scanning confocal microscope (Olympus, Tokyo, Japan).

### 4.8. Chromatin Immunoprecipitation (ChIP) Assay

ChIP assays were performed using a SimpleChIP™ enzymatic chromatin IP kit (Cell Signaling Technology, Danvers, MA, USA). HaCaT cells were seeded in a 100 mm culture dish at $1.5 \times 10^5$ cells/mL, and after 16 h, were treated with 20 µg/mL FFO and 50 µg/mL $PM_{2.5}$. All processes were performed according to the manufacturer's instructions. As an antibody, we used a c-Jun antibody (Invitrogen, Carlsbad, CA, USA). The following primers were designed from the MMP-1 gene promoter (−67 to +94 of the MMP-1 gene sequence from the transcription starting site; Bionics): sense 5′-CCTCTTGCTGCTCCAATATC-3′ and antisense 5′-TCTGCTAGGAGTCACCATTTC-3′. PCR products were separated on 1% agarose gels. DNA bands were photographed under a UV light and were analyzed using Image Quant™ TL analysis software version 1.0.2 (Amersham Biosciences, Uppsala, Sweden).

### 4.9. Statistical Analysis

All analyses were performed in triplicate and all values are expressed as the mean ± standard error of the means. The results were assessed using one-way analysis of variance with Tukey's test using the SigmaStat version 3.5 software (Systat Software Inc., San Jose, CA, USA) to determine the statistical significance of differences between means. A *p*-value < 0.05 was considered to be statistically significant.

**Author Contributions:** Y.J.H. and J.W.H. designed the experiments, and wrote the paper; Y.J.H., M.J.P., K.A.K., A.X.Z., and P.D.S.M.F. performed the experiments; and Y.S.A. and H.K.K. contributed reagents, materials, and analytical tools.

**Conflicts of Interest:** The authors declare no conflict of interest.

## References

1. De Jager, T.L.; Cockrell, A.E.; Du Plessis, S.S. Ultraviolet Light Induced Generation of Reactive Oxygen Species. *Adv. Exp. Med. Biol.* **2017**, *996*, 15–23. [CrossRef] [PubMed]

2. Ryu, O.; Park, B.K.; Bang, M.; Cho, K.S.; Lee, S.H.; Gonzales, E.L.T.; Yang, S.M.; Kim, S.; Eun, P.H.; Lee, J.Y.; et al. Effects of several cosmetic preservatives on ROS-dependent apoptosis of rat neural progenitor cells. *Biomol. Ther.* **2018**, *26*, 608–615. [CrossRef] [PubMed]

3. Abbas, S.; Alam, S.; Pal, A.; Kumar, M.; Singh, D.; Ansari, K.M. UVB exposure enhanced benzanthrone-induced inflammatory responses in SKH-1 mouse skin by activating the expression of COX-2 and iNOS through MAP kinases/NF-κB/AP-1 signalling pathways. *Food Chem. Toxicol.* **2016**, *96*, 183–190. [CrossRef] [PubMed]

4. Ranneh, Y.; Ali, F.; Akim, A.M.; Hamid, H.A.; Khazaai, H.; Fadel, A. Crosstalk between reactive oxygen species and pro-inflammatory markers in developing various chronic diseases: A review. *Appl. Biol. Chem.* **2017**, *60*, 327–338. [CrossRef]

5. Kim, K.H.; Kabir, E.; Kabir, S. A review on the human health impact of airborne particulate matter. *Environ. Int.* **2015**, *74*, 136–143. [CrossRef] [PubMed]

6. Kim, K.E.; Cho, D.; Park, H.J. Air pollution and skin diseases: Adverse effects of airborne particulate matter on various skin diseases. *Life Sci.* **2016**, *152*, 126–134. [CrossRef] [PubMed]

7. Lin, Z.C.; Lee, C.W.; Tsai, M.H.; Ko, H.H.; Fang, J.Y.; Chiang, Y.C.; Liang, C.J.; Hsu, L.F.; Hu, S.C.S.; Yen, F.L. Eupafolin nanoparticles protect HaCaT keratinocytes from particulate matter-induced inflammation and oxidative stress. *Int. J. Nanomed.* **2016**, *11*, 3907–3926. [CrossRef]

8. Seok, J.K.; Lee, J.W.; Kim, Y.M.; Boo, Y.C. Punicalagin and (-)-Epigallocatechin-3-gallate rescue cell viability and attenuate inflammatory responses of human epidermal keratinocytes exposed to airborne particulate matter PM10. *Skin Pharmacol. Physiol.* **2018**, *31*, 134–143. [CrossRef]

9. Chaiprasongsuk, A.; Lohakul, J.; Soontrapa, K.; Sampattavanich, S.; Akarasereenont, P.; Panich, U. Activation of Nrf2 reduces UVA-mediated MMP-1 upregulation via MAPK/AP-1 signaling cascades: The photoprotective effects of sulforaphane and hispidulin. *J. Pharmacol. Exp. Ther.* **2017**, *360*, 388–398. [CrossRef]

10. Kim, J.; Kim, M.B.; Yun, J.G.; Hwang, J.K. Protective effects of standardized siegesbeckia glabrescens extract and its active compound kirenol against UVB-induced photoaging through inhibition of MAPK/NF-κB pathways. *J. Microbiol. Biotechnol.* **2017**, *27*, 242–250. [CrossRef]

11. Leirós, G.J.; Kusinsky, A.G.; Balañá, M.E.; Hagelin, K. Triolein reduces MMP-1 upregulation in dermal fibroblasts generated by ROS production in UVB-irradiated keratinocytes. *J. Dermatol. Sci.* **2017**, *85*, 124–130. [CrossRef] [PubMed]

12. Kim, J.M.; Kim, S.Y.; Noh, E.M.; Song, H.K.; Lee, G.S.; Kwon, K.B.; Lee, Y.R. Reversine inhibits MMP-1 and MMP-3 expressions by suppressing of ROS/MAPK/AP-1 activation in UV-stimulated human keratinocytes and dermal fibroblasts. *Exp. Dermatol.* **2018**, *27*, 298–301. [CrossRef] [PubMed]

13. Xuan, S.H.; Park, Y.M.; Ha, J.H.; Jeong, Y.J.; Park, S.N. The effect of dehydroglyasperin C on UVB-mediated MMPs expression in human HaCaT cells. *Pharmacol. Rep.* **2017**, *69*, 1224–1231. [CrossRef] [PubMed]

14. Pittayapruek, P.; Meephansan, J.; Prapapan, O.; Komine, M.; Ohtsuki, M. Role of matrix metalloproteinases in photoaging and photocarcinogenesis. *Int. J. Mol. Sci.* **2016**, *17*, 868. [CrossRef]

15. Lu, J.; Guo, J.H.; Tu, X.L.; Zhang, C.; Zhao, M.; Zhang, Q.W.; Gao, F.H. Tiron inhibits UVB-induced AP-1 binding sites transcriptional activation on MMP-1 and MMP-3 promoters by MAPK signaling pathway in human dermal fibroblasts. *PLoS ONE* **2016**, *11*, e0159998. [CrossRef]

16. Park, J.E.; Hyun, Y.J.; Piao, M.J.; Kang, K.A.; Ryu, Y.S.; Shilnikova, K.; Zhen, A.X.; Ahn, M.J.; Ahn, Y.S.; Koh, Y.S.; et al. Mackerel-derived fermented fish oil protects skin against UVB-induced cellular damage by inhibiting oxidative stress. *J. Funct. Foods* **2018**, *46*, 147–158. [CrossRef]

17. Gerber, P.A.; Buhren, B.A.; Schrumpf, H.; Hevezi, P.; Bölke, E.; Sohn, D.; Jänicke, R.; Belum, V.R.; Robert, C.; Lacouture, M.E.; et al. Mechanisms of skin aging induced by EGFR inhibitors. *Support Care Cancer* **2016**, *24*, 4241–4248. [CrossRef] [PubMed]

18. Kang, C.H.; Rhie, S.J.; Kim, Y.C. Antioxidant and skin anti-aging effects of marigold methanol extract. *Toxicol. Res.* **2018**, *34*, 31–39. [CrossRef] [PubMed]

19. Avadhani, K.S.; Manikkath, J.; Tiwari, M.; Chandrasekhar, M.; Godavarthi, A.; Vidya, S.M.; Hariharapura, R.C.; Kalthur, G.; Udupa, N.; Mutalik, S. Skin delivery of epigallocatechin-3-gallate (EGCG) and hyaluronic acid loaded nano-transfersomes for antioxidant and anti-aging effects in UV radiation induced skin damage. *Drug Deliv.* **2017**, *24*, 61–74. [CrossRef] [PubMed]

20. Liu, W.H.; Chang, L.S. Caffeine induces matrix metalloproteinase-2 (MMP-2) and MMP-9 down-regulation in human leukemia U937 cells via $Ca^{2+}$/ROS-mediated suppression of ERK/c-fos pathway and activation of p38 MAPK/c-jun pathway. *J. Cell. Physiol.* **2010**, *224*, 775–785. [CrossRef]

21. Kim, M.; Park, Y.G.; Lee, H.J.; Lim, S.J.; Nho, C.W. Youngiasides A and C isolated from Youngia denticulatum inhibit UVB-induced MMP Expression and promote type I procollagen production via repression of MAPK/AP-1/NF-κB and activation of AMPK/Nrf2 in HaCaT cells and human dermal fibroblasts. *J. Agric. Food Chem.* **2015**, *63*, 5428–5438. [CrossRef] [PubMed]

22. Romani, A.; Cervellati, C.; Muresan, X.M.; Belmonte, G.; Pecorelli, A.; Cervellati, F.; Benedusi, M.; Evelson, P.; Valacchi, G. Keratinocytes oxidative damage mechanisms related to airbone particle matter exposure. *Mech. Ageing Dev.* **2018**, *172*, 86–95. [CrossRef] [PubMed]

23. Xing, Y.F.; Xu, Y.H.; Shi, M.H.; Lian, Y.X. The impact of PM2.5 on the human respiratory system. *J. Thorac. Dis.* **2016**, *8*, 69–74. [CrossRef]

24. Subedi, L.; Lee, T.H.; Wahedi, H.M.; Baek, S.H.; Kim, S.Y. Resveratrol-enriched rice attenuates UVB-ROS-induced skin aging via downregulation of inflammatory cascades. *Oxid. Med. Cell. Longev.* **2017**, *2017*, 8379539. [CrossRef] [PubMed]

25. Yoshimoto, S.; Yoshida, M.; Ando, H.; Ichihashi, M. Establishment of photoaging in vitro by repetitive UVA irradiation: Induction of characteristic markers of senescence and its prevention by PAPLAL with potent catalase activity. *Photochem. Photobiol.* **2018**, *94*, 438–444. [CrossRef] [PubMed]

26. Sun, Z.; Park, S.Y.; Hwang, E.; Zhang, M.; Seo, S.A.; Lin, P.; Yi, T.H. Thymus vulgaris alleviates UVB irradiation induced skin damage via inhibition of MAPK/AP-1 and activation of Nrf2-ARE antioxidant system. *J. Cell. Mol. Med.* **2017**, *21*, 336–348. [CrossRef] [PubMed]

27. Hwang, Y.P.; Oh, K.N.; Yun, H.J.; Jeong, H.G. The flavonoids apigenin and luteolin suppress ultraviolet A-induced matrix metalloproteinase-1 expression via MAPKs and AP-1-dependent signaling in HaCaT cells. *J. Dermatol. Sci.* **2011**, *61*, 23–31. [CrossRef] [PubMed]

28. Kim, M.S.; Oh, G.H.; Kim, M.J.; Hwang, J.K. Fucosterol inhibits matrix metalloproteinase expression and promotes type-1 procollagen production in UVB-induced HaCaT cells. *Photochem. Photobiol.* **2013**, *89*, 911–918. [CrossRef] [PubMed]

29. Piao, M.J.; Ahn, M.J.; Kang, K.A.; Ryu, Y.S.; Hyun, Y.J.; Shilnikova, K.; Zhen, A.X.; Jeong, J.W.; Choi, Y.H.; Kang, H.K.; et al. Particulate matter 2.5 damages skin cells by inducing oxidative stress, subcellular organelle dysfunction, and apoptosis. *Arch. Toxicol.* **2018**, *92*, 2077–2091. [CrossRef] [PubMed]

30. Zorin, V.; Zorina, A.; Smetanina, N.; Kopnin, P.; Ozerov, I.V.; Leonov, S.; Isaev, A.; Klokov, D.; Osipov, A.N. Diffuse colonies of human skin fibroblasts in relation to cellular senescence and proliferation. *Aging* **2017**, *9*, 1404–1413. [CrossRef]